Antiviral Research 145 (2017) 146–159

Contents lists available at ScienceDirect

Antiviral Research

journal homepage: www.elsevier.com/locate/antiviral

Interferon-independent antiviral activity of 25-hydroxycholesterol in a teleost fish

Patricia Pereiro [a], Gabriel Forn-Cuní [a], Sonia Dios [a], Julio Coll [b], Antonio Figueras [a], Beatriz Novoa [a, *]

[a] Instituto de Investigaciones Marinas (IIM-CSIC), Vigo, Spain
[b] Department of Biotechnology, Instituto Nacional Investigaciones Agrarias (INIA), Madrid, Spain

ARTICLE INFO

Article history:
Received 13 June 2017
Received in revised form
21 July 2017
Accepted 4 August 2017
Available online 5 August 2017

Keywords:
Zebrafish
Cholesterol 25-hydroxylase
25-Hydroxycholesterol
Antiviral
SVCV
Interferon

ABSTRACT

Oxysterols are a family of cholesterol oxygenated derivatives with diverse roles in many biological activities and have recently been linked with the induction of a cellular antiviral state. The antiviral effects of 25-hydroxycholesterol (25HC) extend to several mammalian enveloped and non-enveloped viruses. It has been reported that the expression of the gene encoding cholesterol 25-hydroxylase (CH25H) is induced by interferons (IFNs). In this work, five *ch25h* genes were identified in the zebrafish (*Danio rerio*) genome. The *ch25h* genes showed different tissue expression patterns and differed in their expression after immune stimulation with lipopolysaccharide (LPS), polyinosinic:polycytidylic acid (PolyI:C) and Spring Viremia Carp Virus (SVCV). Only one of the 5 genes, *ch25hb*, was overexpressed after the administration of the treatments. Synteny and phylogenetic analyses revealed that *ch25hb* is the putative homolog of mammalian *Ch25h* in zebrafish, while the remaining zebrafish *ch25h* genes are products of duplications within the teleost lineage. Interestingly, its modulation was not mediated by type I IFNs, contrasting previous reports on mammalian orthologs. Nevertheless, *in vivo* overexpression of *ch25hb* in zebrafish larvae significantly reduced mortality after SVCV challenge. Viral replication was also negatively affected by 25HC administration to the zebrafish cell line ZF4. In conclusion, the interferon-independent antiviral role of 25HC was extended to a non-mammalian species for the first time, and dual activity that both protects the cells and interacts with the virus cannot be discarded.

1. Introduction

Viruses are known to alter lipid metabolism to favor their own replication by promoting the synthesis of cholesterol and fatty acids (Clark et al., 2012; Greseth and Traktman, 2014; Munger et al., 2008; Sanchez and Dong, 2010; Taylor et al., 2011; Waris et al., 2007; Yu et al., 2011). As a consequence, drugs that affect cellular lipid composition have shown effectiveness in reducing viral replication (Bocchetta et al., 2014; Munger et al., 2008; Rodgers et al., 2012; Ye et al., 2003). Alterations in cholesterol metabolism can also be induced by the host as a defense mechanism against viral infections (Moser et al., 2012; Schoggins and Randall, 2013; Seo et al., 2011).

The membrane-associated enzyme cholesterol 25-hydroxylase (CH25H) is involved in cholesterol and lipid metabolism by catalyzing the formation of 25-hydroxycholesterol (25HC, oxysterol) from cholesterol. Cellular cholesterol levels are regulated through the activity of two transcription factors: the sterol regulatory element binding proteins (SREBPs) and the liver X receptors (LXRs), which control multiple genes implicated in cholesterol biosynthesis and uptake (Horton et al., 2002; Joseph et al., 2002). Soluble oxysterols, such as 25HC, can regulate the activity of the LXR/SREBP signaling pathway by reducing cholesterol synthesis and increasing its efflux and elimination (Accad and Farese, 1998; Janowski et al., 1996; Radhakrishnan et al., 2007). In addition to the well-known metabolic role of oxysterols, some recent publications have reported an antiviral state induced by 25HC against numerous viruses affecting mammals (Anggakusuma et al., 2015; Blanc et al., 2013; Cagno et al., 2017; Civra et al., 2014; Iwamoto et al., 2014; Liu et al., 2013; Shrivastava-Ranjan et al., 2016; Xiang et al., 2015). Interestingly, it was recently observed that herpes simplex virus type 1 is able to reduce CH25H levels by degrading its mRNA due to the endonuclease activity of the viral protein UL41

* Corresponding author.
E-mail address: beatriznovoa@iim.csic.es (B. Novoa).

http://dx.doi.org/10.1016/j.antiviral.2017.08.003
0166-3542/

(You et al., 2017).

Type I interferons (IFNs) are the main cytokines regulating the antiviral innate immune response in vertebrates (Fensterl and Sen, 2009). IFNs induce the expression of a broad array of IFN-stimulated genes (ISG), which encode for proteins with direct antiviral activity, including inhibition of viral transcription, degradation of viral RNA, inhibition of translation or modification of protein function (Sadler and Williams, 2008). In addition, IFNs can alter cellular metabolism at different levels in response to viral infection (Fritsch and Weichhart, 2016). The murine *Ch25h* gene belongs to the group of ISG (Park and Scott, 2010); however, concerning the induction of human *CH25H* by IFNs, two recent publications showed conflicting results (Anggakusuma et al., 2015; Xiang et al., 2015). Independently of *CH25H* induction by IFNs, the expression of this gene is mediated, at least partially, by Toll-like receptor (TLR) activation (Bauman et al., 2009; Diczfalusy et al., 2009; Park and Scott, 2010).

There remains controversy about the immune mechanisms induced by the oxysterol 25HC. Liu et al. (2013) concluded that 25HC inhibits many mammalian enveloped viruses, but not a few non-enveloped viruses, by affecting viral entry through inhibition of virus-cell membrane fusion. Other authors have suggested that 25HC blocks viral growth at the post-entry stage using diverse mechanisms (Anggakusuma et al., 2015; Blanc et al., 2013; Cagno et al., 2017; Shrivastava-Ranjan et al., 2016; Tani et al., 2016; Xiang et al., 2015), and the antiviral effect of 25HC was also extended to certain non-enveloped viruses (Civra et al., 2014). Therefore, 25HC can be effective against specific viruses, but not against others, and it is unclear if a multiplicity of functions could be attributed to 25HC depending on the virus and the cellular state. It has also been reported that 25HC can modulate the immune state of the host at different levels (Cyster et al., 2014; Fessler, 2016). These effects include the suppression of immunoglobulin A (IgA) production by B lymphocytes (Bauman et al., 2009), the differentiation of monocytes into macrophages and activation of phagocytosis (Ecker et al., 2010), the modulation of inflammation (Cagno et al., 2017; Gold et al., 2014; Reboldi et al., 2014) and immune cell migration (Hannedouche et al., 2011; Liu et al., 2011; Yi et al., 2012).

In this work, the complete repertoire of *ch25h* genes was analyzed in the teleost model species zebrafish (*Danio rerio*). Constitutive expression of the *ch25h* genes in different tissues, as well as their induction after treatment with LPS or PolyI:C and infection with SVCV, were analyzed. Only *ch25hb* (*ch25h* localized to chromosome 12), which appears to be the homolog to mammalian CH25H gene, was significantly overexpressed by the tested immune stimuli, and this induction was IFN-independent. *In vivo* overexpression of *ch25hb* reduced the mortality of zebrafish larvae after SVCV infection. Finally, *in vitro* experiments in the zebrafish cell line ZF4 showed that 25HC induces an antiviral state that reduces SVCV replication. This work shows for the first time that 25HC possesses antiviral activity against a non-mammalian virus in a non-mammalian species.

2. Materials and methods

2.1. Gene organization and phylogenetic analysis of zebrafish ch25h genes

The *ch25h* genes were searched in the *Danio rerio* full genome (GRCz10 assembly) (http://www.ensembl.org/Danio_rerio/Info/Index?db=core). Synteny conservation of *ch25h* genes between zebrafish, several teleost species and *Homo sapiens* was analyzed using Genomicus v83.01 (http://www.genomicus.biologie.ens.fr/genomicus-83.01/cgi-bin/search.pl).

The presence of specific domains in the encoded proteins was determined with SMART 4.0 (http://smart.embl.de/) (Letunic et al., 2015) to search sequences for SMART and Pfam (Sonnhammer et al., 1998) domain sets using the HMMER package (Eddy et al., 1995).

For phylogenetic analysis, CH25H protein sequences from representative vertebrate species were retrieved from GenBank and ENSEMBL (www.ensembl.org). The MAFFT online server was used to generate a starting alignment following the E-INS-i strategy (Katoh et al., 2005), which was pruned using Gblocks server 0.91b (Talavera and Castresana, 2007). The best-fitting amino acid replacement model (JTT in this case) was determined using ProtTest 3.2 (Darriba et al., 2011) based on the Akaike Information Criterion (AIC) (Akaike, 1974). Finally, the maximum likelihood gene tree was estimated with PhyML 3.0 (Guindon et al., 2010) and represented in FigTree v1.3.1 (http://tree.bio.ed.ac.uk/software/figtree/). Nodal confidence was calculated and represented using the aLRT method (Anisimova and Gascuel, 2006).

Sequence identity and similarity scores were calculated with the software MatGAT (Campanella et al., 2003) using the BLOSUM62 matrix.

2.2. Fish, virus, cell lines

Adults, embryos and larvae from wild-type zebrafish were obtained from our experimental facility, where zebrafish are maintained following established protocols (Nusslein-Volhard and Dahm, 2002; Westerfield, 2000) (see http://zfin.org/zf_info/zfbook/zfbk.html). Zebrafish were euthanized using a Tricaine methanesulfonate (MS-222) overdose (500 mg/l^{-1}). For microinjection experiments, larvae were anesthetized by adding two drops of a 0.05% MS-222 solution to a Petri plate with a volume of 10 ml of water. Fish care and challenge experiments were reviewed and approved by the CSIC National Committee on Bioethics under approval number ES360570202001/16/FUN01/PAT.05/tipoE/BNG.

The rhabdovirus Spring Viremia of Carp virus (SVCV isolate 56/70) was propagated on Epithelioma Papulosum of Cyprinid (EPC) cells (ATCC CRL-2872) and titrated in 96-well plates. The $TCID_{50}$/ml was calculated according to the Reed and Muench method (Reed and Muench, 1938).

The fibroblastic-like cell line, ZF4, derived from 1-day-old zebrafish embryos (ATCC CRL-2050) (Driever and Rangini, 1993) was cultured in Dulbecco's modified Eagle's medium (DMEM/F12, Gibco) supplemented with 100 μg/ml of primocin (InvivoGen) and 10% fetal bovine serum (FBS) at 26 °C. Human HEK-293 cells (ATCC CRL-1573) (Anisimova and Gascuel, 2006) were grown in Eagle's Minimum Essential Medium (Gibco) supplemented with 100 μg/ml primocin (InvivoGen), 1× non-essential amino acids (Gibco), 1 mM sodium pyruvate (Gibco) and 10% FBS. The cells were incubated in a 5% CO2 atmosphere at 37 °C.

2.3. Plasmid constructions

Zebrafish type I interferon (IFNΦ) *ifnphi1*, *ifnphi2* and *ifnphi3* (GenBank accession numbers: NM207640, NC007114 and NC007114, respectively) expression constructs in the pcDNA3.1 backbone were kindly provided by Dr. Mulero (University of Murcia, Spain).

The *ch25hb* gene was amplified using touchdown PCR (primers in Supplementary Table 1), and the PCR product was cloned using the pcDNA 3.1/V5-His TOPO TA Expression Kit (Invitrogen), but the epitope V5 and the polyhistidine (6xHis) tag were not included. One Shot TOP10F competent cells (Invitrogen) were transformed to generate the plasmid construct (pcDNA 3.1-*ch25hb*). Plasmid purifications were conducted using the PureLink HiPure Plasmid Midiprep Kit (Invitrogen).

2.4. Reagents

25-hydroxycholesterol (25HC), 22(R)-hydroxycholesterol (22(R)HC), cholesterol, LPS and PolyI:C were purchased from Sigma (references H1015, H9384, C8667, L2630 and P9582, respectively).

2.5. Constitutive expression of ch25h genes

The expression of *ch25h* genes under basal conditions was analyzed in different tissues from adult zebrafish. Spleen, liver, kidney, gill and intestine were sampled and pooled, yielding a total of 4 pools of 5 fish per organ. Samples were stored at −80 °C until RNA extraction.

2.6. Zebrafish stimulation with LPS, PolyI:C and SVCV

Adult (9 month) zebrafish were intraperitoneally injected with 10 μl of an SVCV suspension (3×10^6 $TCID_{50}$/ml), and the corresponding controls were injected with the same volume of viral medium (Eagle's minimum essential medium supplemented with 2% fetal bovine serum, penicillin and streptomycin). The same experiment was conducted using LPS (1 mg/ml in PBS; Sigma–L2630) and PolyI:C (1 mg/ml in PBS; Sigma–P1530), and the corresponding controls were injected with PBS. To analyze the induction of *ch25h* transcripts by qPCR, kidneys were sampled from anesthetized fish at 3, 6 and 24 h post-stimulation, and 4 biological replicates (4 fish/replicate) per time point were obtained.

ZF4 cells were seeded on 24-well plates and, at 70–80% confluence, the media was removed and replaced by DMEM + Primocin + 2% FBS containing LPS (50 μg/ml), PolyI:C (50 μg/ml) or SVCV (5×10^4 $TCID_{50}$/ml). Non-treated control wells were also included. The plates were incubated at 27 °C and ZF4 cells were sampled at 3, 6 and 24 h post-stimulation (3 biological replicates per time point).

2.7. Type I IFN in vitro and in vivo assays

To elucidate whether *ch25hb* is an interferon-stimulated gene (ISG) as in mammals, ZF4 cells (2×10^6 cells) were transfected with 15 μg of the expression plasmids pcDNA3.1-*ifnphi1*, pcDNA3.1-*ifnphi2* or pcDNA3.1-*ifnphi3* or the corresponding control vector (pcDNA3.1). Plasmid transfections were carried out using the Neon® Transfection System (Invitrogen) (settings: 1400 V, 20 ms and one electric pulse). Electroporated cells were resuspended in 6 ml of RPMI-1640 Dutch modified (Gibco) medium containing 10% FBS and seeded on 6-well plates (2 wells/treatment). After 72 h, ZF4 cells were collected and stored at −80 °C until RNA isolation.

Supernatant enriched in recombinant zebrafish Ifnphi was produced by transfection of 6 μg the plasmids into HEK-293 cells at 70–80% confluence using the X-tremeGENE HP DNA Transfection Reagent (Roche) according to the manufacturer's instructions. As a control, HEK-293 cells were transfected with the empty plasmid. Forty-eight h after transfection, the supernatants were collected and stored at −80 °C until use. Kidneys from adult zebrafish were aseptically removed and homogenized through a 100-μm mesh, and the mixture was adjusted to the required concentration (1.5×10^6 cells/ml) in Leibovitz L-15 medium (Gibco) supplemented with 100 μg/ml of Primocin (InvivoGen) and 2% FBS and maintained at 26 °C. Kidney primary cells were seeded into 24-well plates at 1 ml per well, and 50 μl of the supernatants containing the recombinant Ifnphi were added to different wells (three wells/treatment). After 4 h of stimulation with the supernatants, the cells were collected for analysis.

The last experiment for confirming that zebrafish *ch25hb* is not induced by type I IFNs was conducted *in vivo*. The recombinant plasmid pcDNA 3.1-*ifnphi1* and the corresponding control (pcDNA 3.1) were microinjected into one-cell stage zebrafish embryos with a glass microneedle using Narishige MN-151 micromanipulator and Narishige IM-30 microinjector. Zebrafish embryos were microinjected with 100 pg/egg (final volume of 2 nl, diluted in PBS) of the recombinant or the empty plasmid. Three days after plasmid infection (3 dpf larvae), three biological replicates of 10 larvae were collected for each treatment.

2.8. Overexpression of ch25hb and protection against SVCV

The pcDNA3.1-*ch25hb* plasmid and the corresponding control (pcDNA3.1) were microinjected into one-cell stage zebrafish embryos as mentioned above. Embryos were microinjected with 150 pg/egg (final volume of 2 nl, diluted in PBS) of plasmids. Three days after plasmid injections (3 dpf larvae), half of the larvae from each treatment were infected into the duct of Cuvier with 2 nl of an SVCV suspension (5×10^4 $TCID_{50}$/ml), and the other half were inoculated with the same volume of PBS. Mortality was assessed during the next three days post-infection (dpi) using three biological replicates composed of 10 larvae each. Samples were also taken after 9 h (5 biological replicates, 10 larvae/replicate) in order to analyze expression of the *ch25hb* gene in non-infected larvae, the viral proliferation in infected larvae, and modulation of the inflammation-related genes *interleukin 6* (*il6*), *interleukin 1 beta* (*il1b*) and *tumor necrosis factor alpha* (*tnfa*), and the ISGs *myxovirus resistance protein 1* (*mxa*), *Interferon-stimulated gene 15* (*isg15*) and *interferon induced protein with tetratricopeptide repeats 17.1* (*ifit17.1*). The primer pairs are listed in Supplementary Table 1.

2.9. Treatment of zebrafish larvae with 25-hydroxycholesterol (25HC)

Zebrafish larvae (2 dpf) were pre-treated with 25HC (50 μg/ml) and 1.25% of the vehicle (ethanol). Control larvae were maintained in 1.25% of ethanol. After 24 h, half of the larvae from each treatment were infected into the duct of Cuvier with 2 nl of an SVCV suspension (5×10^4 $TCID_{50}$/ml), and the other half were inoculated with the same volume of PBS. Mortality was assessed during the next three dpi using three biological replicates composed of 10 larvae each. Samples were also taken after 9 h (5 biological replicates, 10 larvae/replicate) in order to analyze the viral proliferation in infected larvae.

2.10. Treatment of ZF4 cells with different doses of 25HC

ZF4 cells were seeded on 96-well plates and, at 70–80% confluence, the media was removed and replaced by DMEM + Primocin + 2% FBS containing different concentrations (0, 10, 25 and 50 μg/ml) of the oxysterol 25HC and 2.5% of the vehicle (ethanol). After incubation for 20 h at 27 °C, the treatments were removed, the cells were washed twice with PBS and seven 10-fold serial dilutions of SVCV (higher concentration: 1.5×10^5 $TCID_{50}$/ml) in DMEM + Primocin + 2% FBS were used for viral titration in triplicate, following the Reed and Muench method (Reed and Muench, 1938). Non-infected controls were also included. To obtain repetitive results, this experiment was conducted three times. Microscopy images were captured (10× magnification) at 3 dpi with SVCV (1.5×10^3 $TCID_{50}$/ml) using a Nikon Eclipse TS100 inverted microscope.

2.11. Treatment of ZF4 cells with 25HC, 22(R)HC and cholesterol

ZF4 cells were seeded and maintained as mentioned above. Three experimental procedures were performed using 25HC, 22(R)

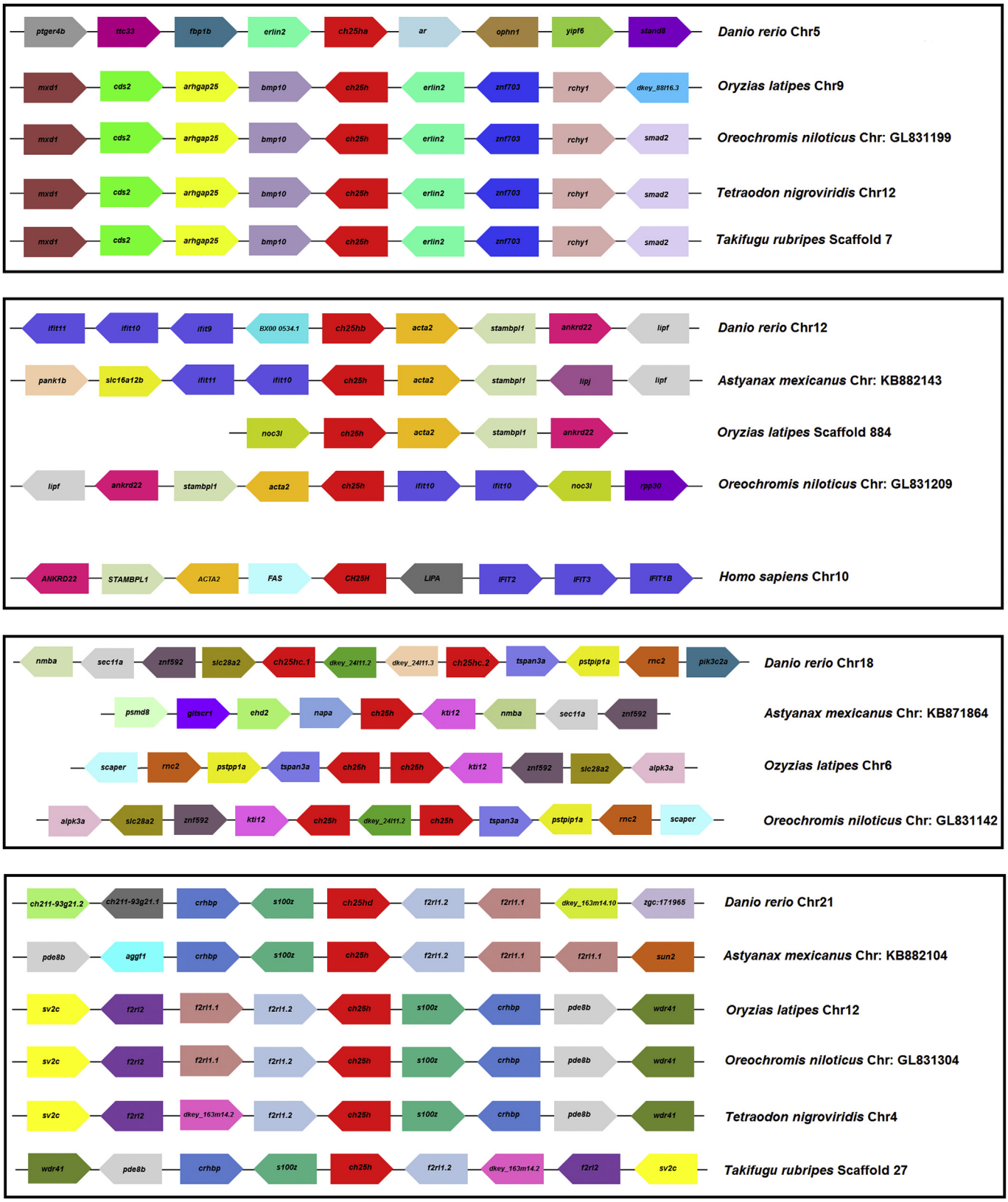

Fig. 1. Synteny analysis of zebrafish *ch25h* genes (red color). Five genes were identified in the zebrafish genome, located on chromosomes 5, 12, 18–2 genes – and 21. The *ch25hb* gene showed synteny conservation with the human *CH25H* gene located on chromosome 10. This gene is located very close, both in humans and teleosts, to members of the IFIT gene family, a group of interferon-stimulated genes (ISGs). The other *D. rerio ch25h* genes also showed a high degree of synteny conservation with other duplicated *ch25h* genes in teleosts.

HC and cholesterol. The experimental designs are graphically represented in Supplementary Fig. 1. In experiment A, ZF4 cell monolayers were pre-treated with 25 μg/ml of 25-HC, 22(R)HC or cholesterol in 2.5% ethanol and then infected with seven 10-fold serial dilutions of SVCV (first concentration: 1.5×10^6 $TCID_{50}$/ml). In experiment B, the cells were pre-incubated with seven 10-fold serial dilutions of SVCV for 2 h, and 25 μg/ml of oxysterols/cholesterol in 2.5% ethanol was then added. Finally, in experiment C, SVCV (1.5×10^6 $TCID_{50}$/ml) was pre-incubated with 25 μg/ml of oxysterols/cholesterol in 2.5% ethanol for 1 h at 27 °C and moderate agitation; then, 10-fold serial dilutions of this mixture were added to the cells. Viral titration was performed following the Reed and Muench method (Reed and Muench, 1938).

24-well plates were also seeded with ZF4 cells, and the conditions for the third SVCV dilution (1.5×10^3 $TCID_{50}$/ml) in the three experiments were replicated. At 24 h post-infection, the media was removed, the cells were washed twice with PBS, RNA was isolated (5 biological replicates) and qPCR was performed for detection of the SVCV N gene. In addition, expression of inflammation-related genes (*il6*, *il1b*, *tnfa*) and ISGs (*mxa*, *isg15*, *ifit17.1*) was also analyzed in the 25HC-treated cells.

2.12. RNA isolation, cDNA synthesis and gene expression analysis

Total RNA isolation was performed using the Maxwell 16 LEV Simply RNA Tissue Kit (Promega, Madison, WI, USA) according to the manufacturer's instructions. cDNA synthesis was performed with SuperScript II Reverse Transcriptase (Invitrogen) using 0.5 μg of RNA. Specific qPCR primers were designed using the Primer3 program (Rozen and Skaletsky, 2000), and their amplification efficiency was calculated using seven serial two-fold dilutions of cDNA from unstimulated zebrafish with the Threshold Cycle (CT) slope method (Pfaffl, 2001). The primer sequences are listed in Supplementary Table 1 qPCR amplifications were performed as previously described (Pereiro et al., 2015). The relative expression level of the genes was normalized using the *18S ribosomal RNA* as reference gene following the Pfaffl method (Pfaffl, 2001).

2.13. Statistical analysis

Kaplan-Meier survival curves were analyzed with a log-Rank (Mantel-Cox) test. Expression results were represented graphically as the means ± standard deviation of the biological replicates.

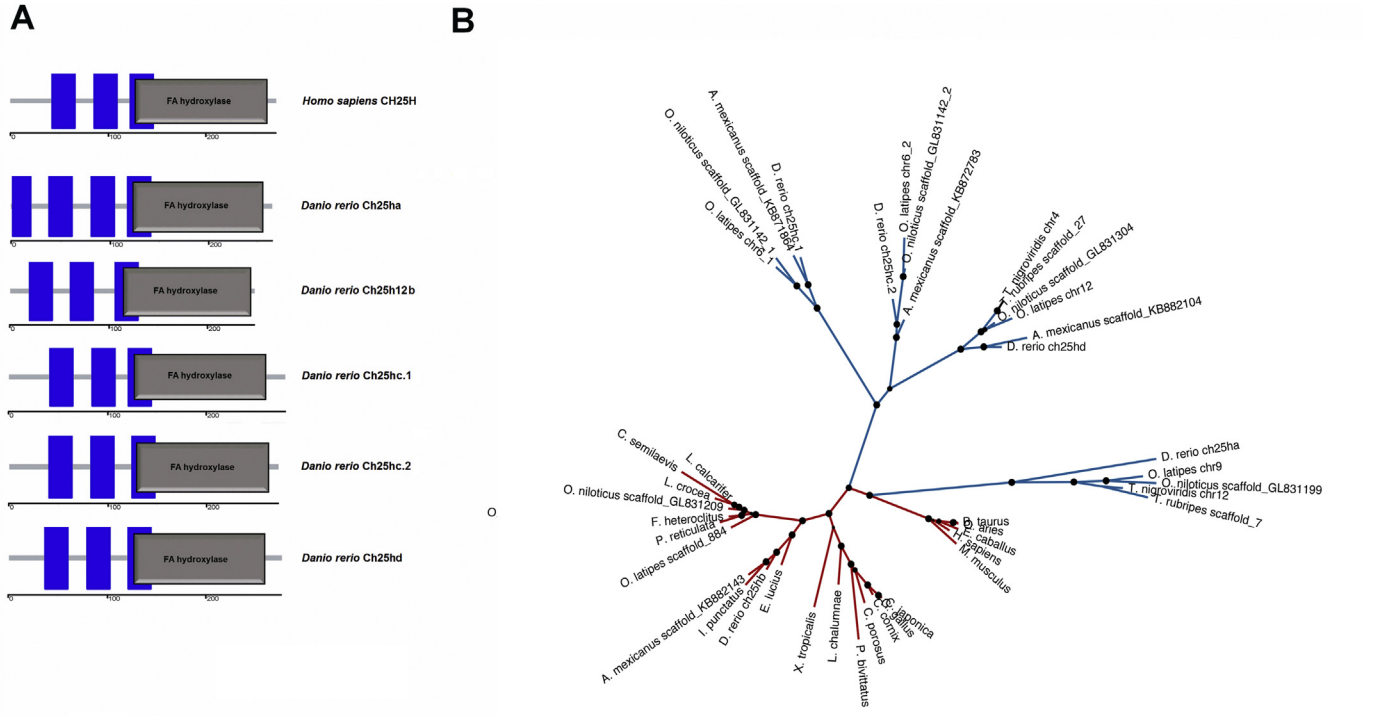

C

	D. rerio ch25ha	*D. rerio* ch25hb	*D. rerio* ch25hc.1	*D. rerio* ch25hc.2	*D. rerio* ch25hd	*H. sapiens* CH25H	*M. musculus* CH25H	*B. taurus* CH25H
***D. rerio* Ch25ha**		40.5	33.4	33.7	29.5	37.6	34.8	39.4
***D. rerio* Ch25hb**	60.2		38.1	45.7	45.5	52.9	48.3	53.0
***D. rerio* Ch25hc.1**	56.0	59.6		45.9	41.3	41.5	40.6	44.0
***D. rerio* Ch25hc.2**	54.0	65.9	66.3		50.4	46.9	44.0	45.1
***D. rerio* Ch25hd**	51.5	69.7	58.9	68.1		42.5	38.7	41.5
***H. sapiens* CH25H**	58.5	68.8	61.3	66.7	62.5		71.1	83.5
***M. musculus* CH25H**	54.7	62.1	61.1	63.4	56.0	79.9		71.5
***B. taurus* CH25H**	61.1	70.7	63.8	67.8	61.1	92.3	79.5	

Fig. 2. Comparative analysis of the CH25H proteins. (A) The presence of specific domains was determined with SMART 4.0. Zebrafish Ch25h proteins present the typical fatty acid hydroxylase domain (grey color). With the exception of Ch25ha, in which four transmembrane domains were predicted, the other zebrafish Ch25h showed three transmembrane domains, as occurs in humans (blue color). (B) A phylogenetic tree reflecting the evolutionary relationships among vertebrate CH25H. The results indicate that Ch25hb is likely the ancient zebrafish Ch25h. (C) An identity/similarity matrix among *D. rerio* Ch25h proteins and their mammalian counterparts was constructed using MatGat software. Zebrafish Ch25hb showed the highest similarity (white) and identity (gray) values with the mammalian proteins.

To determine significant differences, data were analyzed with the computer software package SPSS v.19.0 using Student's t-test or one-way ANOVA with Tukey's post hoc test. Significant differences were displayed as *** ($0.0001 < p < 0.001$), ** ($0.001 < p < 0.01$) or * ($0.01 < p < 0.05$).

2.14. Docking analysis

The N, M1, P, G_{trimer} and L polymerase protein sequences of SVCV were modeled *in silico* from the corresponding 3D vesicular stomatitis virus (VSV) templates (RCSB data bank at http://www.rcsb.org/pdb/home/home.do) by the SWISS-MODEL homology server (https://swissmodel.expasy.org/interactive). The AutoDock Vina (Trott and Olson, 2010) included in the program package PyRx (Dallakyan and Olson, 2015) was used to study the predicted Gibbs free energy of binding (ΔG), using X × Y × Z Å grids surrounding each of the whole protein models. The Gibbs free energies were then converted into predicted inhibition constants in M (Ki), calculated by the formula $Ki = \exp([\Delta G \times 1000]/[R \times T])$ ($R = 1.98$ cal/mol, and $T = 298$) (Shityakov and Forster, 2014). Virtual screen performances were visualized by PyRx and PyMOL.

3. Results

3.1. Gene organization and phylogenetic analysis

At least five *ch25h* genes were discovered in the zebrafish genome distributed on four different chromosomes: one copy on chromosomes 5, 12 and 21, and two copies on chromosome 18. Following the zebrafish gene nomenclature guidelines, we adopted the following gene names: *ch25ha*, *ch25hb*, *ch25hc.1*, *ch25hc.2* and *ch25hd*. The cloned coding sequences were submitted to GenBank with the above-mentioned names under accession numbers MF095413 through MF095417. A high degree of synteny conservation was observed between *D. rerio ch25h* genes and their orthologs in other teleost species (Fig. 1). Even in the case of *ch25hc.1* and *ch25hc.2*, two ortholog genes were also observed positioned in tandem in other fish species, reflecting that these genes are products of an independent duplication that occurred early in the teleost lineage. In contrast, the mammalian genomes only possess one copy of the cholesterol-25-hydroxylase gene. Only the zebrafish *ch25hb* showed synteny conservation with its human homolog, highlighting that this gene copy is probably the original gene of the *ch25h* teleost repertoire.

The exon/intron organization of the zebrafish *ch25h* genes was also analyzed. Only *ch25ha* possesses an intron (>3000 bp), whereas the other four genes are intronless, as in mammals. This gene family encodes proteins composed of 267, 251, 282, 276 and 279 amino acids. All zebrafish Ch25h proteins possess the characteristic fatty acid hydroxylase domain and three transmembrane domains (TMDs), with the exception of Ch25ha, which showed four TMDs (Fig. 2A).

Consistent with synteny studies, the phylogenetic analysis of the CH25H sequence in vertebrates revealed that the zebrafish *ch25hb*

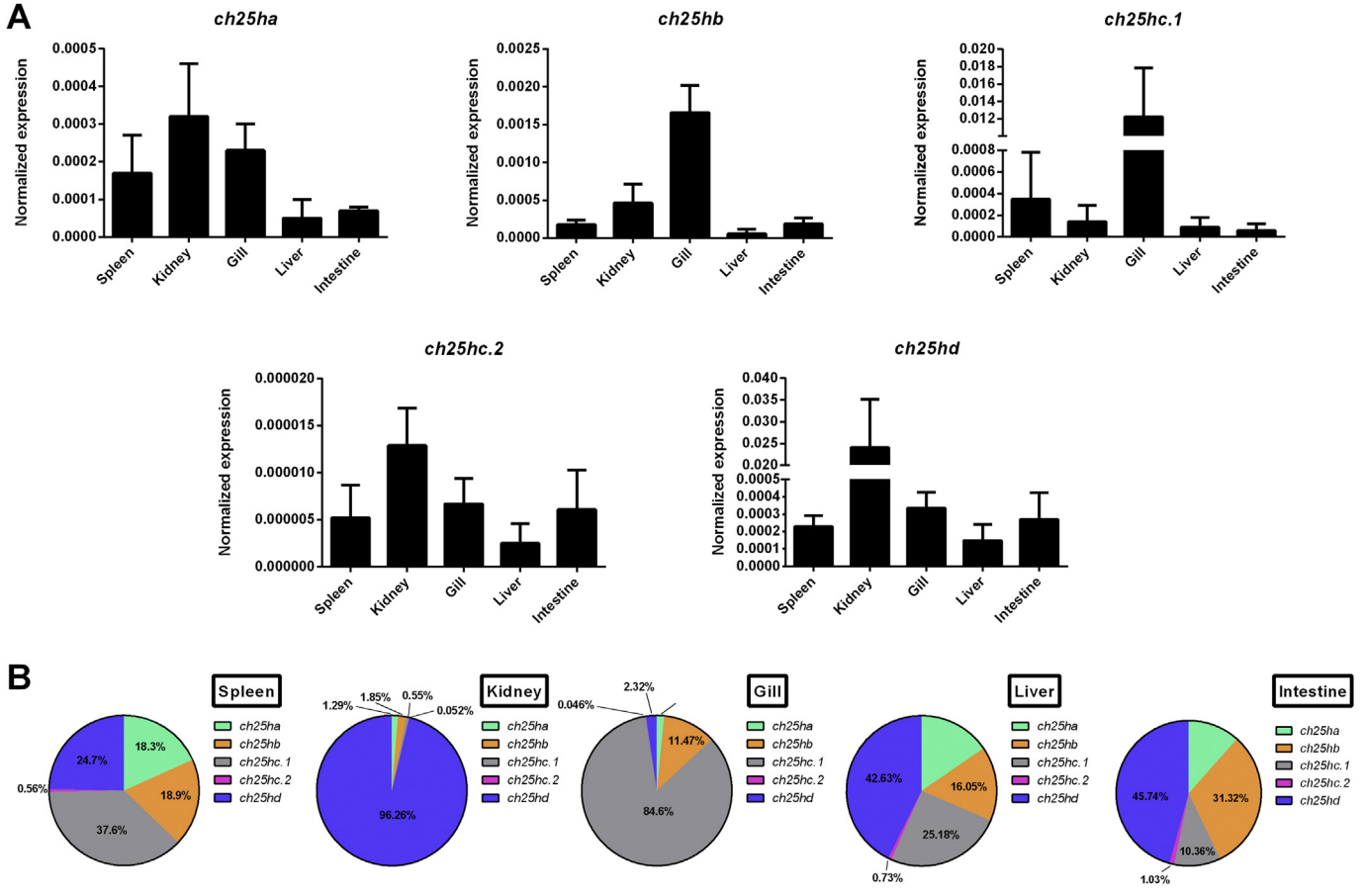

Fig. 3. Tissue expression pattern of *D. rerio ch25h* genes under basal conditions. (A) Normalized expression of *ch25h* genes in the spleen, kidney, gill, liver and intestine of adult zebrafish. The relative expression level of each gene was normalized to the expression of the *18S ribosomal RNA* gene in the same tissue. The graphs represent the means ± standard deviation of 4 independent biological replicates. (B) Relative proportion (%) of the *ch25h* transcripts in different zebrafish tissues.

gene is the one consistent with the species evolution, while the remaining zebrafish ortholog Ch25h sequences were grouped together with other fish-specific proteins derived from gene duplications in external branches (Fig. 2B). A similarity/identity matrix also reflected this higher homology of *D. rerio* Ch25hb with its mammalian counterparts (Fig. 2C).

3.2. Basal expression pattern of zebrafish ch25h genes

The constitutive expression of the five *ch25h* genes was analyzed in different tissues from healthy adult zebrafish (Fig. 3). *ch25ha, ch25hc.2* and *ch25hd* showed an identical pattern, being highly expressed in the kidney followed by the gill, spleen, intestine and liver; in the case of *ch25hd*, the difference between the kidney and the other tissues was much higher (Fig. 3A). On the other hand, *ch25hb* and *ch25hc.1* were mainly expressed in the gill (Fig. 3A).

ch25hd was the predominant transcript in the kidney (96% of the total), liver (43%) and intestine (46%), but *ch25hc.1* was the most expressed in the spleen (38%) and gill (85%) (Fig. 3B). In contrast, *ch25hc.2* was the lowest expressed gene in the tested tissues.

3.3. Induction of different ch25h genes after immune stimulation

Three different immune stimulators (LPS, PolyI:C and SVCV) were delivered by intraperitoneal injection in adult zebrafish. Transcription of the *ch25h* repertoire was analyzed in the main immune tissue in fish, the kidney, at different times after injection (3, 6 and 24 h) (Fig. 4). While *ch25ha* was not affected by any of the treatments, reductions in the transcription of *ch25hc.1*, *ch25hc.2* and *ch25hd* were observed with different stimuli. Only *ch25hb* was overexpressed following the three stimuli. LPS induced a moderate and sustained overexpression of *ch25hb* at the tested times post-challenge (fold changes −FC−: 3.6, 2.8 and 4.1). Whereas PolyI:C induced a time-decreasing modulation (FC: 16.9, 6.2, 3.1), *ch25hb* was only significantly modulated by SVCV 24 h after infection (FC: 17.3).

In ZF4 cells, the stimuli did not induce any significant difference in the expression of *ch25h* genes compared to the controls (Supplementary Fig. 2A). Under constitutive conditions, *ch25hb* showed the highest transcription level in this cell type (Supplementary Fig. 2B).

3.4. Expression of ch25hb is not modulated by type I IFN treatment

Different experiments were conducted in order to elucidate whether or not zebrafish *ch25hb* is an interferon-stimulated gene (ISG), as previously reported in mammals.

The transfection of ZF4 cells with the expression plasmids encoding zebrafish type I IFNs (pcDNA3.1-*ifnphi1*, pcDNA 3.1-*ifnphi2*, pcDNA 3.1-*ifnphi3*) revealed a significant induction of ISGs (*mxa* and *ifit17.1*) after 72 h; this was in contrast to the transcription of *ch25hb*, which was not affected (Fig. 5A). On the other hand, the conditioned supernatants from HEK-293 cells transfected with the corresponding IFN-coding plasmids induced the expression of zebrafish *interferon-induced proteins with tetratricopeptide repeats* (*ifit)* in kidney primary cell cultures 4 h post-stimulation, as was previously reported (data not shown) (Varela et al., 2014). In contrast, using these same samples, *ch25hb* was not modulated by recombinant IFNs (Fig. 5B). Finally, the microinjection of pcDNA3.1-*ifnphi1* into one-cell stage zebrafish embryos revealed a significant induction of *mxa* and *ifit17.1* in the resulting larvae after 3 days, but *ch25hb* transcription was unaffected (Fig. 5C). Together, these results show that zebrafish *ch25hb* is not modulated by zebrafish type I IFNs and therefore is not an ISG.

3.5. ch25hb overexpression reduces the mortality and viral replication after an SVCV challenge

Zebrafish embryos were microinjected with an expression plasmid construction containing the *ch25hb* gene (pcDNA3.1-*ch25hb*) or with the corresponding empty plasmid (pcDNA3.1) as a control. The efficiency of the plasmid was determined by analyzing the correct transcription of the *ch25hb* gene three days after injection. A 127-fold increase in *ch25hb* transcript levels was detected compared to the larvae injected with the empty plasmid (Fig. 6A). At 3 days post-fertilization (dpf), larvae were challenged with SVCV or PBS (negative control) microinjection into the duct of Cuvier in order to induce a systemic infection. Differences in the viral replication were analyzed by detecting the SVCV nucleoprotein (N) gene 9 h post-infection (hpi). A significant reduction in the detection of the N gene was observed in those larvae previously microinjected with pcDNA3.1-*ch25hb* compared to the individuals receiving the empty plasmid (Fig. 6B). Mortality recorded during the next three

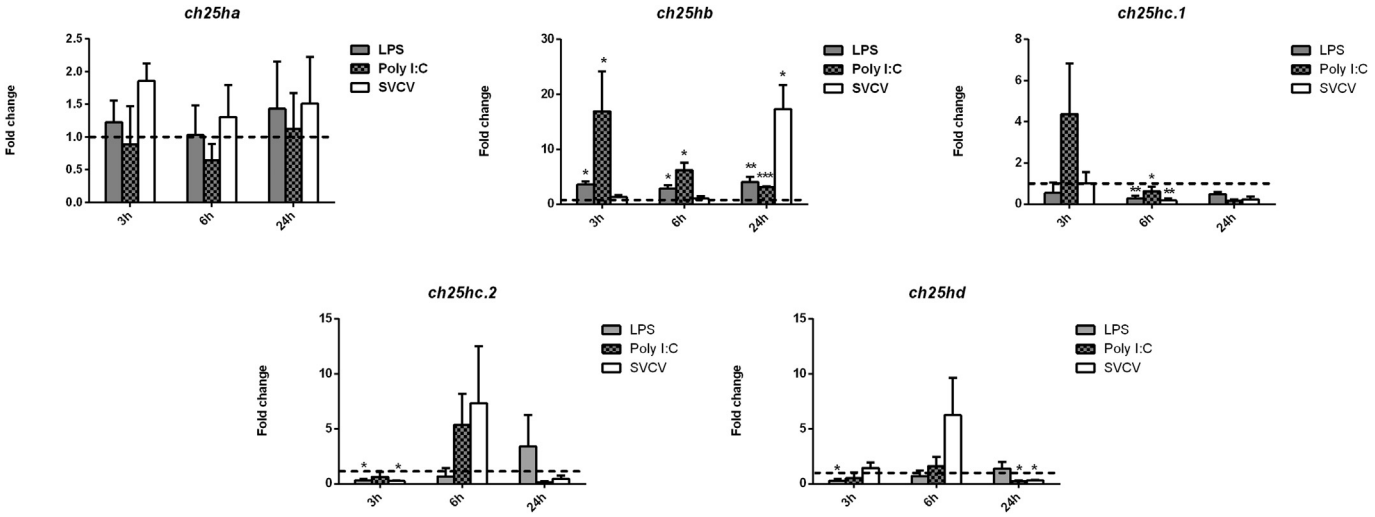

Fig. 4. *ch25h* gene modulation in the kidney of adult zebrafish at 3, 6 and 24 h after LPS, PolyI:C or SVCV challenge. The expression level of each gene was normalized to the expression of the *18S ribosomal RNA* gene and expressed as the fold change with respect to the levels detected in the control group (PBS-injected). The graphs represent the means ± standard deviation of 4 independent biological replicates. Significant differences are displayed as *** ($0.0001 < p < 0.001$), ** ($0.001 < p < 0.01$) or * ($0.01 < p < 0.05$).

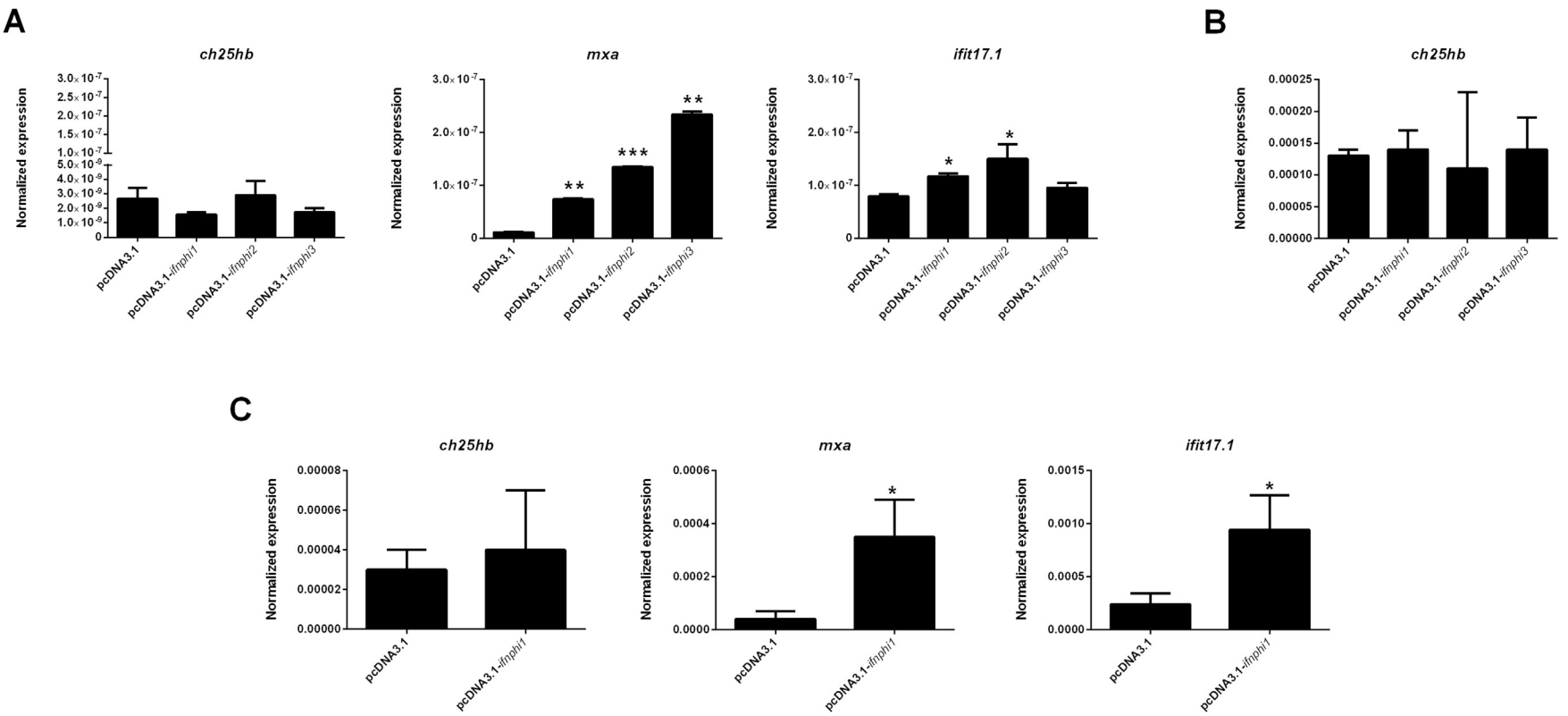

Fig. 5. Effect of type I interferons on the induction of *ch25hb*. (A) The expression plasmids encoding zebrafish i*fnphi1*, *ifnphi2* and *ifnphi3* were transfected into ZF4 cells. After 3 days, the expression of *ch25hb* was analyzed. Whereas two typical ISGs (*mxa* and *ifit17.1*) were found to be overexpressed after IFN stimulations, *ch25hb* was not significantly affected. The relative expression level of each gene was normalized to the expression of the *18S ribosomal RNA* gene. The graphs represent the means ± standard deviation of 2 biological replicates. (B) Recombinant zebrafish Ifnphi was produced in HEK-293 cells, and primary kidney cells were stimulated with this protein. The expression of *ch25hb* was analyzed after 4 h, and any significant modulation was observed. These samples were previously used to analyze the expression of the zebrafish IFIT family, and significant overexpression of these ISGs was observed (Varela et al., 2014). The relative expression level of *ch25hb* was normalized to the expression of the *18S ribosomal RNA* gene. The graph represents the means ± standard deviation of 3 biological replicates. (C) One-cell stage zebrafish embryos were microinjected with the expression plasmid encoding *ifnphi1* or the corresponding empty plasmid. After 3 days, the expression of *ch25hb* was not significantly affected, whereas *mxa* and *ifit17.1* were overexpressed. The relative expression level of each gene was normalized to the expression of the *18S ribosomal RNA* gene. The graphs represent the means ± standard deviation of 3 biological replicates. In the three cases, significant differences are displayed as *** ($0.0001 < p < 0.001$), ** ($0.001 < p < 0.01$) or * ($0.01 < p < 0.05$).

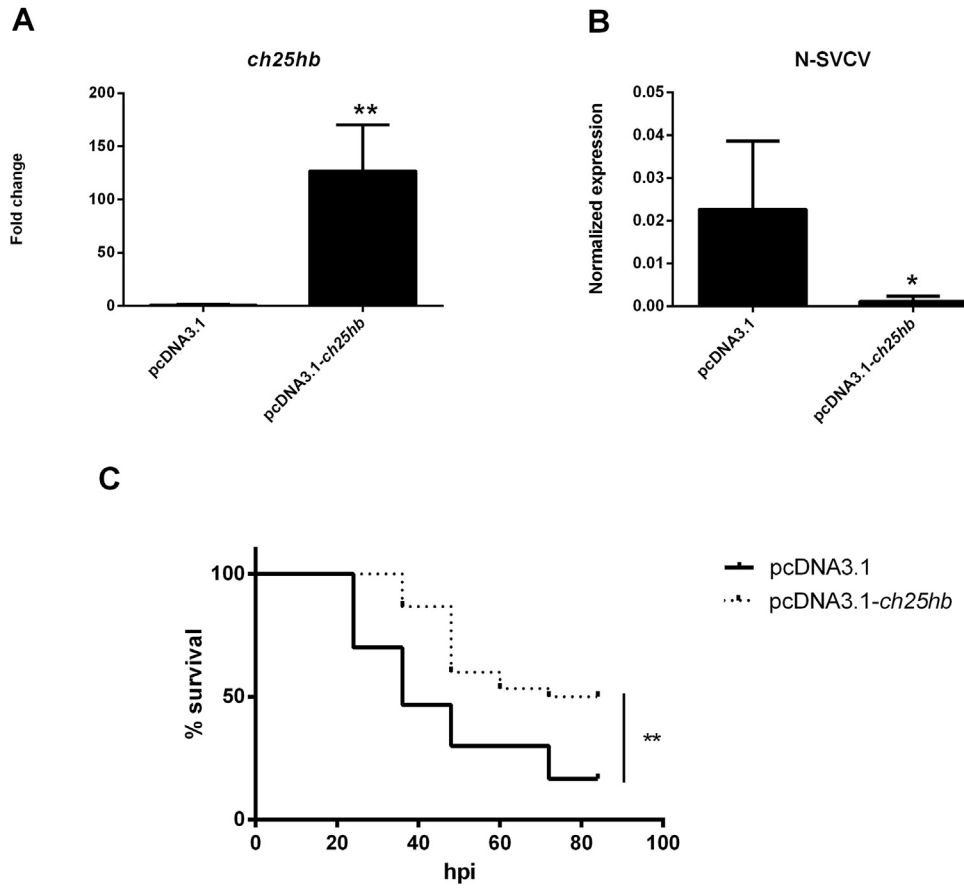

Fig. 6. *In vivo ch25hb* overexpression reduces the mortality rate after SVCV infection. (A) Expression of *ch25hb* in 3 dpf zebrafish larvae microinjected in one-cell stage embryos with pcDNA3.1-*ch25hb* or the empty plasmid (pcDNA3.1). The expression level of *ch25hb* was normalized to the expression of the *18S ribosomal RNA* gene and expressed as the fold change with respect to the level detected in the control group (pcDNA3.1-injected). *ch25hb* was overexpressed 127-fold in the individuals receiving the expression plasmid. The graph represents the means ± standard deviation of 5 independent biological replicates. (B) Detection of the SVCV nucleoprotein (N) gene 9 h post-infection in larvae previously receiving the plasmid pcDNA3.1-*ch25hb* or pcDNA3.1. A significant reduction in viral detection was observed in individuals in which *ch25hb* was overexpressed. The expression level of N-SVCV was normalized to the expression of the *18S ribosomal RNA* gene. The graph represents the means ± standard deviation of 5 independent biological replicates. (C) Kaplan-Meier survival curves after infection with 2 nl of an SVCV solution in zebrafish larvae overexpressing or not *ch25hb*. Significant differences are displayed as *** ($0.0001 < p < 0.001$), ** ($0.001 < p < 0.01$) or * ($0.01 < p < 0.05$).

days showed that the injection with the plasmid pcDNA3.1-*ch25hb* increased the survival after SVCV infection (Fig. 6C). However, zebrafish larvae exposed to 25HC prior to infection with SVCV did not show significant differences in survival (Supplementary Fig. 3A) and viral detection (Supplementary Fig. 3B) compared to non-treated larvae.

Additionally, the expression of the inflammatory-related genes *il6*, *il1b* and *tnfa*, and the ISGs *mxa*, *isg15* and *ifit17.1* was analyzed by quantitative PCR (qPCR) in the absence and presence of infection. No significant differences were observed between the individuals receiving the empty plasmid and those microinjected with the expression plasmid pMCV1.4-*ch25hb* (Supplementary Fig. 4).

3.6. Reduction of SVCV replication by 25HC treatment

Different concentrations of 25HC were used to test its antiviral effect after pre-incubation with ZF4 monolayers. Even the lower dose of 25HC used (10 μg/ml) was able to induce a 0.78-logarithm (log) reduction in virus titer, whereas 1-log was obtained for the higher doses (Fig. 7A). Microscopy images taken 3 days post-infection (dpi) showed a reduction of the cytopathic effect (CPE) in those cells pre-incubated with 25 μg/ml 25HC (Fig. 7B).

The expression of *il6*, *il1b*, *tnfa*, *mxa*, *isg15* and *ifit17.1* was also measured in non-treated and 25HC-treated ZF4 cells 24 h post-infection. Only a significant reduction in the transcription of *tnfa* was observed in those cells previously treated with 25HC in the absence of infection (Supplementary Fig. 5). After SVCV infection, *ifit17.1* was significantly higher expressed in ZF4 cells previously receiving 25HC compared to non-treated cells (Supplementary Fig. 3).

For studying the specificity of the antiviral effect of 25HC, 22(R)-hydroxycholesterol (22(R)HC) and cholesterol were also tested. Three different types of experiments were performed: A) Pre-incubation with oxysterols/cholesterol for 20 h followed by washing and SVCV infection; B) Infection with SVCV for 2 h followed by washing and treatment with oxysterols/cholesterol; C) Pre-incubation of oxysterols/cholesterol with SVCV for 1 h followed by addition of the mixtures to the cell monolayers. In experiment A, the viral titer was reduced by 4-logs compared to the non-treated control both with 25HC and 22(R)HC oxysterols, but no differences with the control were observed for the cholesterol treatment (Fig. 8A). The level of the SVCV N gene at 24 h post-infection was lower in those cells previously incubated with the oxysterols (Fig. 8B). In experiment B, the viral titer was also reduced by 4-logs with 25HC, whereas any CPE was observed in the ZF4 cells treated with 22(R)HC (Fig. 8A); in both cases, the level of the SVCV N gene was significantly reduced (Fig. 8B). In the last assay, experiment C, a small reduction of 1-log was accompanied by lower SVCV N gene

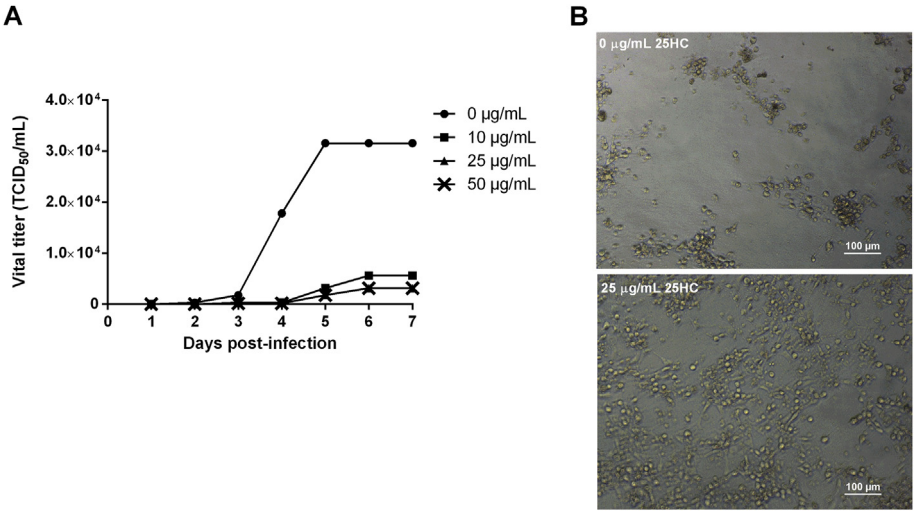

Fig. 7. 25-hydroxycholesterol (25HC) reduces SVCV replication in the ZF4 cell line. (A) ZF4 cells were pre-incubated for 20 h with different concentrations of 25HC. Then, the cells were infected with 1:10 serial dilutions of SVCV. Evolution of the CPE was checked every day, and the viral titer was calculated following the Reed and Muench method. A reduction of 1-log in the viral titer was detected for the higher doses. (B) Microscopy images showing the state of the ZF4 cells at 3 days post-infection (SVCV: 1.5×10^3 $TCID_{50}$/mL). An evident protective effect of 25HC was observed.

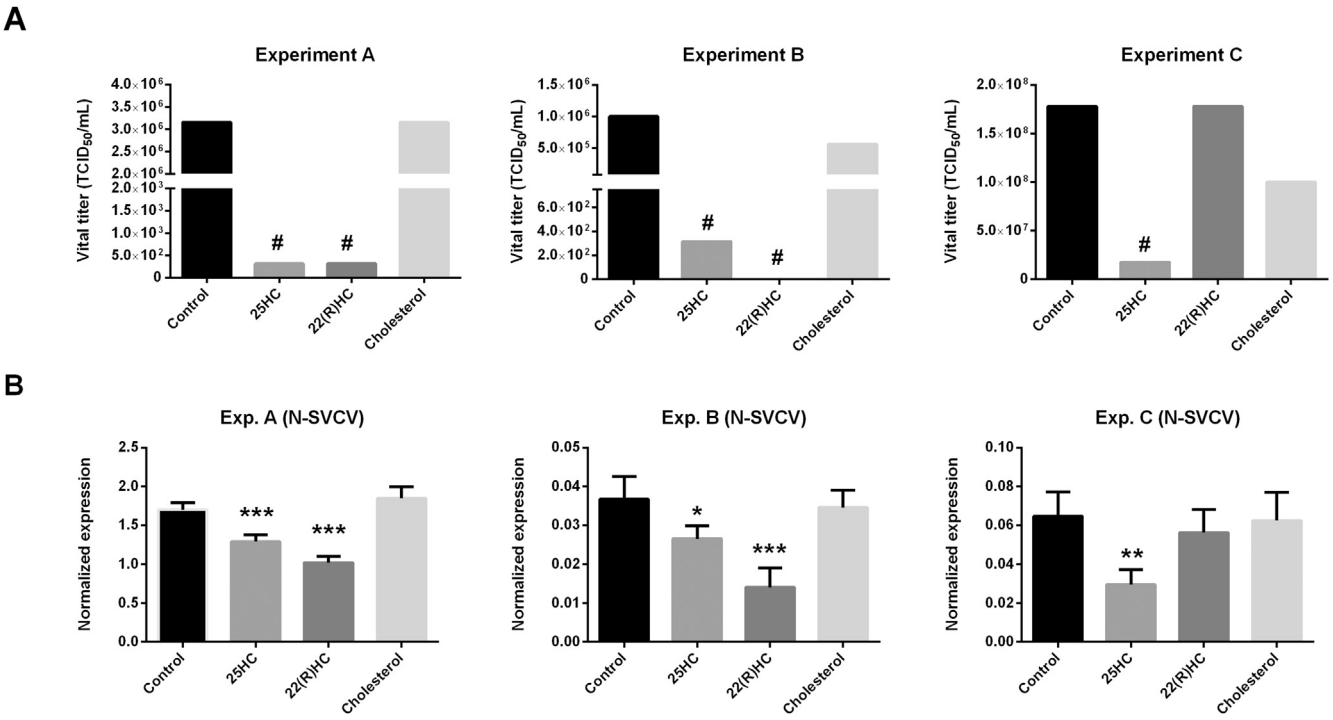

Fig. 8. Antiviral effect of oxysterols against SVCV using different experimental approaches. In experiment A, ZF4 cells were pre-incubated for 20 h with 25 µg/ml of 25HC, 22(R)HC or cholesterol before the infection. In experiment B, the cells were first infected with SVCV for 2 h, and the different treatments were then added. Finally, in experiment C, serial dilutions of SVCV and oxysterols/cholesterol were pre-incubated for 1 h and then added to the cells. (A) Both 25HC and 22(R)HC induced a ≥1-log reduction in the viral titer in experiment A and B. Nevertheless, in experiment C, only 25HC induced a ≥1-log reduction in the viral titer. Hashes (#) indicate viral titer reductions ≥1-log. (B) Detection of the SVCV N gene in ZF4 cells 24 h post-infection in the conditions corresponding to the third viral dilution (1.5×10^3 $TCID_{50}$/mL). Significant reductions in SVCV replication were observed for 25HC and 22(R)HC in experiments A and B, whereas only 25HC reduced the viral load in experiment C. The expression level of N-SVCV was normalized to the expression of the *18S ribosomal RNA* gene. The graph represents the means ± standard deviation of 5 biological replicates. Significant differences are displayed as *** ($0.0001 < p < 0.001$), ** ($0.001 < p < 0.01$) or * ($0.01 < p < 0.05$).

levels only with 25HC (Fig. 8A and B). The absence of SVCV inhibition by 22(R)HC and the moderate but significant effect of 25HC in this last experiment suggest the probability of a direct interaction between 25HC and the SVCV proteins.

3.7. Docking simulations of oxysterol/cholesterol-SVCV interactions

To explore the existence of potential interactions of the oxysterols and cholesterol with SVCV, its N, M1, M2, G and L protein virion sequences were *in silico* modeled from the corresponding 3D

vesicular stomatitis virus (VSV) templates (RCSB data bank at http://www.rcsb.org/pdb/home/home.do) using the SWISS-MODEL homology server (https://swissmodel.expasy.org/interactive). The lowest values for the predicted docking interactions were for the L polymerase (0.08–0.21 μM) compared to the rest of the SVCV proteins (Fig. 9, lower table). The corresponding binding sites on the L protein showed that, while 22(R)HC and cholesterol were located on the external part (amino acids 1450–1455) of the connector domain (Liang et al., 2015), 25HC was located on the internal methyltransferase domain (amino acid stretches 1885–1900 and 1755–1760) (Fig. 9, upper figure). These results suggest that, despite its lower binding energy, 22(R)HC and cholesterol could be bound by the virions without inactivating them, whereas 25HC could also inhibit the methylation of the RNA by steric hindrance in addition to other mechanisms. This hypothesis offers a possible explanation for the absence of SVCV inhibition when the virus is mixed with 22(R)HC and cholesterol before infection (Fig. 8, experiment C). However, it is not yet known whether this structural *in silico* prediction may be the definitive explanation for the results obtained *in vitro*.

4. Discussion

Oxysterols are multifunctional molecules with a recently identified connection to antiviral immunity in mammals. 25HC, produced from cholesterol due to the activity of the enzyme CH25H, is one of the most studied oxysterols in this sense, and its antiviral activity has been reported against numerous viruses (Anggakusuma et al., 2015; Blanc et al., 2013; Cagno et al., 2017; Civra et al., 2014; Liu et al., 2013; Shrivastava-Ranjan et al., 2016; Tani et al., 2016; Xiang et al., 2015). In this work, we characterized the repertoire of *ch25h* genes in the zebrafish animal model. Fish homologs of mammalian genes are usually duplicated through its genome due to fish-specific, additional genome duplication (3R) that is hypothesized to have occurred 350 million years ago (Meyer and Van de Peer, 2005) in the teleost lineage. Consequently, numerous copies of *ch25h* are present in the zebrafish genome, whereas only one copy exists in mammals. Among the five zebrafish *ch25h* genes, the one on chromosome 12, *ch25hb*, appears to be the true homolog to the mammalian *CH25H* gene, as evidenced by synteny, phylogenetic and identity/similarity analyses.

These five genes showed differential tissue expression profiles, indicating that they likely evolved to acquire complementary or specialized functions. Indeed, although *ch25hb* is not the most expressed *ch25h* gene copy in the head kidney – the main immune tissue in fish – it was the only gene copy that was found to be significantly overexpressed in this tissue after LPS, PolyI:C or SVCV administration. The induction of *ch25hb* by LPS administration was previously observed in zebrafish larvae (Dios et al., 2014), similarly to the *Ch25h* gene in mouse macrophages (Diczfalusy et al., 2009). Modulation of this gene seems to be, at least in part, TLR-mediated (Bauman et al., 2009; Diczfalusy et al., 2009; Park and Scott, 2010). It is interesting to highlight that, in mammals, LPS is specifically recognized by TLR4, but this gene is absent or is not sensitive to LPS in teleosts, suggesting an alternative but unclear inflammatory activation pathway in response to LPS (Forn-Cuní et al., 2017) that leads to the *ch25hb* transcription modulation.

Ch25h has typically been described as an ISG in mammals (Anggakusuma et al., 2015; Park and Scott, 2010), but a recent publication reported that, whereas *Ch25h* is overexpressed after IFN-beta treatment in murine bone marrow-derived dendritic cells, this is not observed in human hepatocytes after treatments with IFN-alpha, IFN-beta, IFN-gamma or IFN-lambda; therefore, it seems that *Ch25h* is not a typical ISG (Xiang et al., 2015). While the

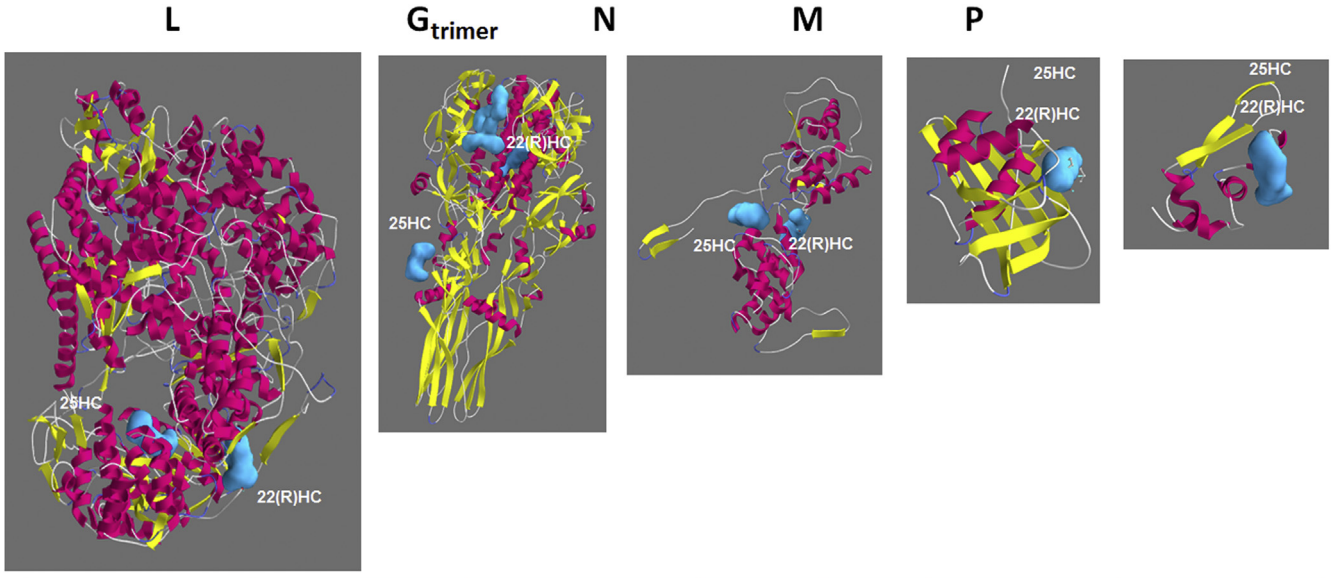

μM	L	G_{trimer}	N	M	P
25HC	0.08	4.41	1.90	2.66	12.16
22(R)HC	0.21	7.32	1.14	3.15	46.96
Ch	0.96	20.18	1.14	4.41	65.83

Fig. 9. Docking simulations of oxysterol/cholesterol with SVCV protein 3D models. The 22(R)HC and cholesterol best bindings located on the external part of the L polymerase (amino acids 1450–1455) into the L connector domain (44), while 25HC was located in the internal methyltransferase domain (amino acid stretches 1885–1900 and 1755–1760). Red, predicted α-helixes. Yellow, predicted β-sheets. Solid blue, oxysterol/cholesterol molecules bound to the SVCV protein models.

complete repertoire of zebrafish *ch25h* genes was not analyzed, *ch25hb* induction is not mediated by type I IFN overexpression. Therefore, the pathway inducing the transcription of this gene remains to be elucidated. Interestingly, synteny analysis revealed that *ch25hb* and the corresponding orthologs in other teleost species and humans are located in tandem with members of the IFIT family, which belong to the group of ISGs (Varela et al., 2014). It is very common that genes controlled by the same transcription factors form tandem gene clusters in the genomes (Boldogköi, 2012), although we cannot discard a loss of IFN-mediated activation during the evolution of the different taxonomic groups. Although a putative IFN-stimulated response element (ISRE) has been identified in the *ch25hb* promoter with the sequence AACTTTCAGTTTTCC, this transcription element is located in a distal position from the ATG start codon (−1821 bp upstream). It has been previously reported that many distal ISREs are not functional (Ronni et al., 1998; Rutherford et al., 1988; Shi et al., 2013; Williams, 1991).

As mentioned above, a broad antiviral activity of CH25H and its product, 25HC, has been demonstrated in murine and human cells. However, the exact mechanism providing this antiviral state is not clear. The inhibition of viral entry (Liu et al., 2013) and post-entry immune processes (Anggakusuma et al., 2015; Blanc et al., 2013; Cagno et al., 2017; Shrivastava-Ranjan et al., 2016; Xiang et al., 2015; Tani et al., 2016) were recently proposed. Across different studies, the post-entry activity has been completely or partially attributed to alterations of the mevalonate pathway (Blanc et al., 2013), blockage of membranous web formation (Anggakusuma et al., 2015), aberrant glycosylation of the viral glycoprotein through unknown mechanisms or the induction of a pro-inflammatory state (Cagno et al., 2017). Numerous immune effects are attributed to 25HC, including the suppression of the production of IgA by B lymphocytes (Bauman et al., 2009), the differentiation of monocytes to macrophages and phagocytosis (Ecker et al., 2010), modulation of inflammation in different ways (Cagno et al., 2017; Gold et al., 2014; Reboldi et al., 2014) and immune cell migration (Hannedouche et al., 2011; Liu et al., 2011; Yi et al., 2012). However, with the exception of Cagno et al. (2017), who found that 25HC promotes the production of IL-6 after herpes simplex-1 virus infection, the relationship of these immune mechanisms with the antiviral activity of 25HC has not been reported. Our results do not show any significant difference in the expression of the inflammation-related genes *il6*, *il1b* and *tnfa* in zebrafish larvae previously microinjected with pcDNA3.1-*ch25hb*, although a slight but significant downregulation in the level of *tnfa* was observed in ZF4 cells treated with 25HC. This is not the first time that the levels/activity of TNF-alpha have been linked with cholesterol-derived molecules or with cholesterol metabolism itself (Cohen-Lahav et al., 2006; Field et al., 2010; Fon Tacer et al., 2007; 2010; Spillmann et al., 2014; Xu et al., 2012), and we cannot rule out that this downregulation in *tnfa* transcription is contributing to the antiviral state induced by 25HC. Contrasting with the results obtained by Cagno et al. (2017), the levels of *il6* were found to be downregulated after SVCV challenge in both *in vivo* and *in vitro* experiments, and no effect due to *ch25hb* overexpression or direct 25HC treatment was observed. In addition to this, no significant differences were observed in the expression of ISGs with the exception of *ifit17.1*, which was higher expressed after SVCV challenge in ZF4 cells previously incubated with 25HC. However, this could be due to the higher ability of the host to mount an effective antiviral response as a consequence of the lower viral load.

In this work, we demonstrate that overexpression of the enzyme Ch25hb reduces the mortality after SVCV infection in zebrafish larvae, indicating that the CH25H antiviral role is conserved in teleosts. However, probably due to low incorporation of the product, the 25HC did not present this activity. Nevertheless, *in vitro* assays in ZF4 cells using the oxysterols 25HC and 22(R)HC reflected the antiviral effect of both oxysterols. Although the reduction of virus replication was higher using 22(R)HC in some cases, this oxysterol was ineffective when SVCV was pre-incubated with the oxysterol. Nevertheless, 25HC was able to reduce the viral titer by 1-log and significantly reduce the SVCV detection 24 h post-infection when SVCV was pre-incubated with 25HC, albeit with a lower viral inhibition compared to the other *in vitro* experiments. Therefore, we cannot discard a direct effect of 25HC on viral viability, which was not observed for 22(R)HC. Shrivastava-Ranjan et al. (2016) provided evidence that 25HC inhibits glycosylation of the Lassa virus (LASV) glycoprotein; as consequence, its infectivity is reduced. Although these authors proposed that Golgi-complex and *trans*-Golgi network-associated glycosylases and/or mannosidases involved in glycoprotein maturation might be affected by 25HC (Shrivastava-Ranjan et al., 2016), a direct interaction of 25HC with the viral proteins could be occurring. Taking this into consideration, docking simulations were conducted in order to analyze the potential interactions between the oxysterols and cholesterol with the SVCV proteins. The results indicate that the potential binding site of 25HC with the L protein could be affecting the correct methylation of the viral RNA. In conclusion, antiviral activity of both 25HC and 22(R)HC against SVCV was observed when the oxysterols were added before or after infection, suggesting an inhibitory activity unrelated to direct interaction with SVCV virions. However, a direct interaction of 25HC or 22(R)HC with the virions, resulting in the presence or absence of an antiviral effect, respectively, cannot be excluded.

5. Conclusions

Five *ch25h* genes were identified in the zebrafish genome, which showed differential tissue expression profiles and modulation abilities after LPS, PolyI:C and SVCV challenges. Only *ch25hb*, the putative homolog of mammalian *Ch25h*, was significantly overexpressed after the intraperitoneal injection of the three stimuli. Nevertheless, our studies revealed that this induction is independent of type I IFNs. The overexpression of *ch25hb* in zebrafish larvae significantly reduced the SVCV replication and mortality during a systemic infection. Moreover, the oxysterol 25HC reduced the viral titer in ZF4 cells using different experimental approaches, and a direct effect of 25HC in the virion infectivity cannot be discarded. Further investigation is needed in order to fully elucidate this aspect.

Acknowledgments

This work was funded by the projects AGL2014-53190-REDT and AGL2014−51773-C3 from the Spanish Ministerio de Economía y Competitividad and IN607B 2016/12 from Consellería de Economía, Emprego e Industria (GAIN), Xunta de Galicia. The funders had no role in the study design, data collection and interpretation or the decision to submit the work for publication.

Appendix A. Supplementary data

Supplementary data related to this article can be found at http://dx.doi.org/10.1016/j.antiviral.2017.08.003.

References

Accad, M., Farese Jr., R.V., 1998. Cholesterol homeostasis: a role for oxysterols. Curr. Biol. 8, R601−R604.
Akaike, H., 1974. A new look at the statistical model identification. IEEE Trans.

Autom. Contr. 19, 716–723.
Anggakusuma, Romero-Brey, I., Berger, C., Colpitts, C.C., Boldanova, T., Engelmann, M., Todt, D., Perin, P.M., Behrendt, P., Vondran, F.W., Xu, S., Goffinet, C., Schang, L.M., Heim, M.H., Bartenschlager, R., Pietschmann, T., Steinmann, E., 2015. Interferon-inducible cholesterol-25-hydroxylase restricts hepatitis C virus replication through blockage of membranous web formation. Hepatology 62, 702–714.
Anisimova, M., Gascuel, O., 2006. Approximate likelihood-ratio test for branches: a fast, accurate, and powerful alternative. Syst. Biol. 55, 539–552.
Bauman, D.R., Bitmansour, A.D., McDonald, J.G., Thompson, B.M., Liang, G., Russell, D.W., 2009. 25-Hydroxycholesterol secreted by macrophages in response to Toll-like receptor activation suppresses immunoglobulin A production. Proc. Natl. Acad. Sci. U. S. A. 106, 16764–16769.
Blanc, M., Hsieh, W.Y., Robertson, K.A., Kropp, K.A., Forster, T., Shui, G., Lacaze, P., Watterson, S., Griffiths, S.J., Spann, N.J., Meljon, A., Talbot, S., Krishnan, K., Covey, D.F., Wenk, M.R., Craigon, M., Ruzsics, Z., Haas, J., Angulo, A., Griffiths, W.J., Glass, C.K., Wang, Y., Ghazal, P., 2013. The transcription factor STAT-1 couples macrophage synthesis of 25-hydroxycholesterol to the interferon antiviral response. Immunity 38, 106–118.
Bocchetta, S., Maillard, P., Yamamoto, M., Gondeau, C., Douam, F., Lebreton, S., Lagaye, S., Pol, S., Helle, F., Plengpanich, W., Guérin, M., Bourgine, M., Michel, M.L., Lavillette, D., Roingeard, P., le Goff, W., Budkowska, A., 2014. Up-regulation of the ATP-binding cassette transporter A1 inhibits hepatitis C virus infection. PLoS One 9, e92140.
Boldogköi, Z., 2012. Transcriptional interference networks coordinate the expression of functionally related genes clustered in the same genomic loci. Front. Genet. 3, 122.
Cagno, V., Civra, A., Rossin, D., Calfapietra, S., Caccia, C., Leoni, V., Dorma, N., Biasi, F., Poli, G., Lembo, D., 2017. Inhibition of herpes simplex-1 virus replication by 25-hydroxycholesterol and 27-hydroxycholesterol. Redox Biol. 12, 522–527.
Campanella, J.J., Bitincka, L., Smalley, J., 2003. MatGAT: an application that generates similarity/identity matrices using protein or DNA sequences. BMC Bioinforma. 4, 29.
Civra, A., Cagno, V., Donalisio, M., Biasi, F., Leonarduzzi, G., Poli, G., Lembo, D., 2014. Inhibition of pathogenic non-enveloped viruses by 25-hydroxycholesterol and 27-hydroxycholesterol. Sci. Rep. 4, 7487.
Clark, P.J., Thompson, A.J., Vock, D.M., Kratz, L.E., Tolun, A.A., Muir, A.J., McHutchison, J.G., Subramanian, M., Millington, D.M., Kelley, R.I., Patel, K., 2012. Hepatitis C virus selectively perturbs the distal cholesterol synthesis pathway in a genotype-specific manner. Hepatology 56, 49–56.
Cohen-Lahav, M., Shany, S., Tobvin, D., Chaimovitz, C., Douvdevani, A., 2006. Vitamin D decreases NFkappaB activity by increasing IkappaBalpha levels. Nephrol. Dial. Transpl. 21, 889–897.
Cyster, J.G., Dang, E.V., Reboldi, A., Yi, T., 2014. 25-Hydroxycholesterols in innate and adaptive immunity. Nat. Rev. Immunol. 14, 731–743.
Dallakyan, S., Olson, A.J., 2015. Small-molecule library screening by docking with PyRx. Methods Mol. Biol. 1263, 243–250.
Darriba, D., Taboada, G.L., Doallo, R., Posada, D., 2011. ProtTest 3: fast selection of best-fit models of protein evolution. Bioinformatics 27, 1164–1165.
Diczfalusy, U., Olofsson, K.E., Carlsson, A.M., Gong, M., Golenbock, D.T., Rooyackers, O., Fläring, U., Björkbacka, H., 2009. Marked upregulation of cholesterol 25-hydroxylase expression by lipopolysaccharide. J. Lipid Res. 50, 2258–2264.
Dios, S., Balseiro, P., Costa, M.M., Romero, A., Boltaña, S., Roher, N., Mackenzie, S., Figueras, A., Novoa, B., 2014. The involvement of cholesterol in sepsis and tolerance to lipopolysaccharide highlighted by the transcriptome analysis of zebrafish (*Danio rerio*). Zebrafish 11, 421–433.
Driever, W., Rangini, Z., 1993. Characterization of a cell line derived from zebrafish (*Brachydanio rerio*) embryos. In Vitro Cell. Dev. Biol. Anim. 29A, 749–754.
Ecker, J., Liebisch, G., Englmaier, M., Grandl, M., Robenek, H., Schmitz, G., 2010. Induction of fatty acid synthesis is a key requirement for phagocytic differentiation of human monocytes. Proc. Natl. Acad. Sci. U. S. A. 107, 7817–7822.
Eddy, S.R., Mitchison, G., Durbin, R., 1995. Maximum discrimination hidden Markov models of sequence consensus. J. Comput. Biol. 2, 9–23.
Fensterl, V., Sen, G.C., 2009. Interferons and viral infections. Biofactors 35, 14–20.
Fessler, M.B., 2016. The intracellular cholesterol landscape: dynamic integrator of the immune response. Trends Immunol. 37, 819–830.
Field, F.J., Watt, K., Mathur, S.N., 2010. TNF-alpha decreases ABCA1 expression and attenuates HDL cholesterol efflux in the human intestinal cell line Caco-2. J. Lipid Res. 51, 1407–1415.
Fon Tacer, K., Kuzman, D., Seliskar, M., Pompon, D., Rozman, D., 2007. TNF-alpha interferes with lipid homeostasis and activates acute and proatherogenic processes. Physiol. Genomics 31, 216–227.
Fon Tacer, K., Pompon, D., Rozman, D., 2010. Adaptation of cholesterol synthesis to fasting and TNF-alpha: profiling cholesterol intermediates in the liver, brain, and testis. J. Steroid Biochem. Mol. Biol. 121, 619–625.
Forn-Cuní, G., Varela, M., Pereiro, P., Novoa, B., Figueras, A., 2017. Conserved gene regulation during acute inflammation between zebrafish and mammals. Sci. Rep. 7, 41905.
Fritsch, S.D., Weichhart, T., 2016. Effects of interferons and viruses on metabolism. Front. Immunol. 7, 630.
Gold, E.S., Diercks, A.H., Podolsky, I., Podyminogin, R.L., Askovich, P.S., Treuting, P.M., Aderem, A., 2014. 25-Hydroxycholesterol acts as an amplifier of inflammatory signaling. Proc. Natl. Acad. Sci. U. S. A. 111, 10666–10671.
Greseth, M.D., Traktman, P., 2014. De novo fatty acid biosynthesis contributes significantly to establishment of a bioenergetically favorable environment for vaccinia virus infection. PLoS Pathog. 10, e1004021.
Guindon, S., Dufayard, J.F., Lefort, V., Anisimova, M., Hordijk, W., Gascuel, O., 2010. New algorithms and methods to estimate Maximum-Likelihood phylogenies: assessing the performance of PhyML 3.0. Syst. Biol. 59, 307–321.
Hannedouche, S., Zhang, J., Yi, T., Shen, W., Nguyen, D., Pereira, J.P., Guerini, D., Baumgarten, B.U., Roggo, S., Wen, B., Knochenmuss, R., Noël, S., Gessier, F., Kelly, L.M., Vanek, M., Laurent, S., Preuss, I., Miault, C., Christen, I., Karuna, R., Li, W., Koo, D.I., Suply, T., Schmedt, C., Peters, E.C., Falchetto, R., Katopodis, A., Spanka, C., Roy, M.O., Detheux, M., Chen, Y.A., Schultz, P.G., Cho, C.Y., Seuwen, K., Cyster, J.G., Sailer, A.W., 2011. Oxysterols direct immune cell migration via EBI2. Nature 475, 524–527.
Horton, J.D., Goldstein, J.L., Brown, M.S., 2002. SREBPs: activators of the complete program of cholesterol and fatty acid synthesis in the liver. J. Clin. Invest. 109, 1125–1131.
Iwamoto, M., Watashi, K., Tsukuda, S., Aly, H.H., Fukasawa, M., Fujimoto, A., Suzuki, R., Aizaki, H., Ito, T., Koiwai, O., Kusuhara, H., Wakita, T., 2014. Evaluation and identification of hepatitis B virus entry inhibitors using HepG2 cells overexpressing a membrane transporter NTCP. Biochem. Biophys. Res. Commun. 443, 808–813.
Janowski, B.A., Willy, P.J., Devi, T.R., Falck, J.R., Mangelsdorf, D.J., 1996. An oxysterol signaling pathway mediated by the nuclear receptor LXR alpha. Nature 383, 728–731.
Joseph, S.B., Laffitte, B.A., Patel, P.H., Watson, M.A., Matsukuma, K.E., Walczak, R., Collins, J.L., Osborne, T.F., Tontonoz, P., 2002. Direct and indirect mechanisms for regulation of fatty acid synthase gene expression by liver X receptors. J. Biol. Chem. 277, 11019–11025.
Katoh, K., Kuma, K., Toh, H., Miyata, T., 2005. MAFFT version 5: improvement in accuracy of multiple sequence alignment. Nucleic Acids Res. 33, 511–518.
Letunic, I., Doerks, T., Bork, P., 2015. SMART: recent updates, new developments and status in 2015. Nucleic Acids Res. 43, D257–D260.
Liang, B., Li, Z., Jenni, S., Rahmeh, A.A., Morin, B.M., Grant, T., Grigorieff, N., Harrison, S.C., Whelan, S.P., 2015. Structure of the L protein of vesicular stomatitis virus from electron cryomicroscopy. Cell 162, 314–327.
Liu, C., Yang, X.V., Wu, J., Kuei, C., Mani, N.S., Zhang, L., Yu, J., Sutton, S.W., Qin, N., Banie, H., Karlsson, L., Sun, S., Lovenberg, T.W., 2011. Oxysterols direct B-cell migration through EBI2. Nature 475, 519–523.
Liu, S.Y., Aliyari, R., Chikere, K., Li, G., Marsden, M.D., Smith, J.K., Pernet, O., Guo, H., Nusbaum, R., Zack, J.A., Freiberg, A.N., Su, L., Lee, B., Cheng, G., 2013. Interferon-inducible cholesterol-25-hydroxylase broadly inhibits viral entry by production of 25-hydroxycholesterol. Immunity 38, 92–105.
Meyer, A., Van de Peer, Y., 2005. From 2R to 3R: evidence for a fish-specific genome duplication (FSGD). BioEssays 27, 937–945.
Moser, T.S., Schieffer, D., Cherry, S., 2012. AMP-activated kinase restricts Rift Valley fever virus infection by inhibiting fatty acid synthesis. PLoS Pathog. 8, e1002661.
Munger, J., Bennett, B.D., Parikh, A., Feng, X.J., McArdle, J., Rabitz, H.A., Shenk, T., Rabinowitz, J.D., 2008. Systems-level metabolic flux profiling identifies fatty acid synthesis as a target for antiviral therapy. Nat. Biotechnol. 26, 1179–1186.
Nusslein-Volhard, C., Dahm, R., 2002. Zebrafish, a Practical Approach. Oxford University Press, Oxford.
Park, K., Scott, A.L., 2010. Cholesterol 25-hydroxylase production by dendritic cells and macrophages is regulated by type I interferons. J. Leukoc. Biol. 88, 1081–1087.
Pereiro, P., Varela, M., Diaz-Rosales, P., Romero, A., Dios, S., Figueras, A., Novoa, B., 2015. Zebrafish Nk-lysins: first insights about their cellular and functional diversification. Dev. Comp. Immunol. 51, 148–159.
Pfaffl, M.W., 2001. A new mathematical model for relative quantification in real-time RT-PCR. Nucleic Acids Res. 29, 2002–2007.
Radhakrishnan, A., Ikeda, Y., Kwon, H.J., Brown, M.S., Goldstein, J.L., 2007. Sterol-regulated transport of SREBPs from endoplasmic reticulum to Golgi: oxysterols block transport by binding to Insig. Proc. Natl. Acad. Sci. U. S. A. 104, 6511–6518.
Reboldi, A., Dang, E.V., McDonald, J.G., Liang, G., Russell, D.W., Cyster, J.G., 2014. Inflammation. 25-Hydroxycholesterol suppresses interleukin-1-driven inflammation downstream of type I interferon. Science 345, 679–684.
Reed, L.J., Muench, H., 1938. A simple method of estimating fifty percent endpoints. Am. J. Hyg. 27, 493–497.
Rodgers, M.A., Villareal, V.A., Schaefer, E.A., Peng, L.F., Corey, K.E., Chung, R.T., Yang, P.L., 2012. Lipid metabolite profiling identifies desmosterol metabolism as a new antiviral target for hepatitis C virus. J. Am. Chem. Soc. 134, 6896–6899.
Ronni, T., Matikainen, S., Lehtonen, A., Palvimo, J., Dellis, J., Van Eylen, F., Goetschy, J.F., Horisberger, M., Content, J., Julkunen, I., 1998. The proximal interferon-stimulated response elements are essential for interferon responsiveness: a promoter analysis of the antiviral MxA gene. J. Interferon Cytokine Res. 18, 773–781.
Rozen, S., Skaletsky, H., 2000. Primer3 on the WWW for general users and for biologist programmers. Methods Mol. Biol. 132, 365–386.
Rutherford, M.N., Hannigan, G.E., Williams, B.R., 1988. Interferon-induced binding of nuclear factors to promoter elements of the 2-5A synthetase gene. EMBO J. 7, 751–759.
Sadler, A.J., Williams, B.R.G., 2008. Interferon-inducible antiviral effectors. Nat. Rev. Immunol. 8, 559–568.
Sanchez, V., Dong, J.J., 2010. Alteration of lipid metabolism in cells infected with human cytomegalovirus. Virology 404, 71–77.
Schoggins, J.W., Randall, G., 2013. Lipids in innate antiviral defense. Cell Host Microbe 14, 379–385.

Seo, J.Y., Yaneva, R., Cresswell, P., 2011. Viperin: a multifunctional, interferon-inducible protein that regulates virus replication. Cell Host Microbe 10, 534–539.
Shi, J., Zhang, Y.B., Zhang, J.S., Gui, J.F., 2013. Expression regulation of zebrafish interferon regulatory factor 9 by promoter analysis. Dev. Comp. Immunol. 4, 534–543.
Shityakov, S., Forster, C., 2014. In silico predictive model to determine vector-mediated transport properties for the blood-brain barrier choline transporter. Adv. Appl. Bioinform. Chem. 7, 23–36.
Shrivastava-Ranjan, P., Bergeron, É., Chakrabarti, A.K., Albariño, C.G., Flint, M., Nichol, S.T., Spiropoulou, C.F., 2016. 25-hydroxycholesterol inhibition of Lassa virus infection through aberrant GP1 glycosylation. MBio 7, e01808–e01816.
Sonnhammer, E.L., Eddy, S.R., Birney, E., Bateman, A., Durbin, R., 1998. Pfam: multiple sequence alignments and HMM-profiles of protein domains. Nucleic Acids Res. 26, 320–322.
Spillmann, F., Van Linthout, S., Miteva, K., Lorenz, M., Stangl, V., Schultheiss, H.P., Tschöpe, C., 2014. LXR agonism improves TNF-α-induced endothelial dysfunction in the absence of its cholesterol-modulating effects. Atherosclerosis 232, 1–9.
Talavera, G., Castresana, J., 2007. Improvement of phylogenies after removing divergent and ambiguously aligned blocks from protein sequence alignments. Syst. Biol. 56, 564–577.
Tani, H., Shimojima, M., Fukushi, S., Yoshikawa, T., Fukuma, A., Taniguchi, S., Morikawa, S., Saijo, M., 2016. Characterization of glycoprotein-mediated entry of severe fever with thrombocytopenia syndrome virus. J. Virol. 90, 5292–5301.
Taylor, H.E., Linde, M.E., Khatua, A.K., Popik, W., Hildreth, J.E., 2011. Sterol regulatory element-binding protein 2 couples HIV-1 transcription to cholesterol homeostasis and T cell activation. J. Virol. 85, 7699–7709.
Trott, O., Olson, A.J., 2010. AutoDock Vina: improving the speed and accuracy of docking with a new scoring function, efficient optimization, and multithreading. J. Comput. Chem. 31, 455–461.
Varela, M., Diaz-Rosales, P., Pereiro, P., Forn-Cuní, G., Costa, M.M., Dios, S., Romero, A., Figueras, A., Novoa, B., 2014. Interferon-induced genes of the expanded IFIT family show conserved antiviral activities in non-mammalian species. PLoS ONE 9, e100015.
Waris, G., Felmlee, D.J., Negro, F., Siddiqui, A., 2007. Hepatitis C virus induces proteolytic cleavage of sterol regulatory element binding proteins and stimulates their phosphorylation via oxidative stress. J. Virol. 81, 8122–8130.
Westerfield, M., 2000. The Zebrafish Book. A Guide for the Laboratory Use of Zebrafish (*Danio rerio*), fourth ed. University of Oregon Press, Eugene.
Williams, B.R.G., 1991. Transcriptional regulation of interferon-stimulated genes. Eur. J. Biochem. 200, 1–11.
Xiang, Y., Tang, J.J., Tao, W., Cao, X., Song, B.L., Zhong, J., 2015. Identification of cholesterol 25-hydroxylase as a novel host restriction factor and a part of the primary innate immune responses against hepatitis C virus infection. J. Virol. 89, 6805–6816.
Xu, L., Shen, S., Ma, Y., Kim, J.K., Rodriguez-Agudo, D., Heuman, D.M., Hylemon, P.B., Pandak, W.M., Ren, S., 2012. 25-Hydroxycholesterol-3-sulfate attenuates inflammatory response via PPARγ signaling in human THP-1 macrophages. Am. J. Physiol. Endocrinol. Metab. 302, E788–E799.
Ye, J., Wang, C., Sumpter Jr., R., Brown, M.S., Goldstein, J.L., Gale Jr., M., 2003. Disruption of hepatitis C virus RNA replication through inhibition of host protein geranylgeranylation. Proc. Natl. Acad. Sci. U. S. A. 100, 15865–15870.
Yi, T., Wang, X., Kelly, L.M., An, J., Xu, Y., Sailer, A.W., Gustafsson, J.A., Russell, D.W., Cyster, J.G., 2012. Oxysterol gradient generation by lymphoid stromal cells guides activated B cell movement during humoral responses. Immunity 37, 535–548.
You, H., Yuan, H., Fu, W., Su, C., Wang, W., Cheng, T., Zheng, C., 2017. Herpes simplex virus type 1 abrogates the antiviral activity of Ch25h via its virion host shutoff protein. Antivir. Res. 143, 69–73.
Yu, Y., Clippinger, A.J., Alwine, J.C., 2011. Viral effects on metabolism: changes in glucose and glutamine utilization during human cytomegalovirus infection. Trends Microbiol. 19, 360–367.